

Charge Delocalization in a Homologous Series of α,α' -Bis(dianisylamino)-Substituted Thiophene Monocations

Journal:	<i>The Journal of Physical Chemistry</i>
Manuscript ID:	jp-2012-03989t.R1
Manuscript Type:	Article
Date Submitted by the Author:	31-May-2012
Complete List of Authors:	Reuter, Luisa; University of Goettingen, Institute of Inorganic Chemistry Bonn, Annabell; University of Goettingen, Institute of Inorganic Chemistry Stückl, A. Claudia; University of Goettingen, Institute of Inorganic Chemistry He, Bice; Universität Göttingen, Chemistry Pati, Palas; Indian Institute of Science Education and Research, Kolkata, Department of Chemical Sciences Zade, Sanjio; Indian Institute of Science Education and Research, Kolkata, Department of Chemical Sciences Wenger, Oliver; University of Goettingen, Institute of Inorganic Chemistry

SCHOLARONE™
Manuscripts

1
2
3
4
5
6
7
8
9
10
11
12
13
14
15
16
17
18
19
20
21
22
23
24
25
26
27
28
29
30
31
32
33

Charge Delocalization in a Homologous Series of α,α' - Bis(dianisylamino)-Substituted Thiophene Monocations

Luisa G. Reuter,[†] Annabell G. Bonn,[†] A. Claudia Stückl,[†] Bice He,[†] Palas Baran Pati,[‡] Sanjio S. Zade,[‡]
Oliver S. Wenger^{*,†}

[†]Georg-August-Universität Göttingen, Institut für Anorganische Chemie, Tammannstrasse 4, D-37077
Göttingen, Germany

[‡] Department of Chemical Sciences, Indian Institute of Science Education and Research, Kolkata, PO:
BCKV Campus Main Office, Mohanpur 741252, Nadia, West Bengal, India

oliver.wenger@chemie.uni-goettingen.de

34
35
36
37
38
39
40

**RECEIVED DATE (to be automatically inserted after your manuscript is accepted if required
according to the journal that you are submitting your paper to)**

41
42
43
44
45
46
47
48
49
50
51
52
53
54
55
56
57
58
59
60

ABSTRACT

A homologous series of three molecules containing thiophene, bithiophene and terthiophene bridges between two redox-active tertiary amino-groups was synthesized and explored. Charge-delocalization in the one-electron oxidized forms of these molecules was investigated by a combination of cyclic voltammetry, near-infrared optical absorption spectroscopy, and EPR spectroscopy. All three cation radicals can be described as organic mixed-valence species, and for all of them the experimental data is consistent with strong delocalization of the unpaired electron. Depending on what model is used for

1 analysis of the optical absorption data, estimates for the electronic coupling matrix element (H_{AB}) range
2 from $\sim 5000 \text{ cm}^{-1}$ to $\sim 7000 \text{ cm}^{-1}$ for the shortest member of the homologous series. According to optical
3 absorption and EPR spectroscopy even the terthiophene radical appears to belong either to Robin-Day
4 class III or to a category of radicals commonly denominated as borderline class II / class III systems. The
5 finding of such a large extent of charge delocalization over up to three adjacent thiophene units is
6 remarkable.
7
8
9
10
11
12
13
14
15
16
17
18

19 KEYWORDS

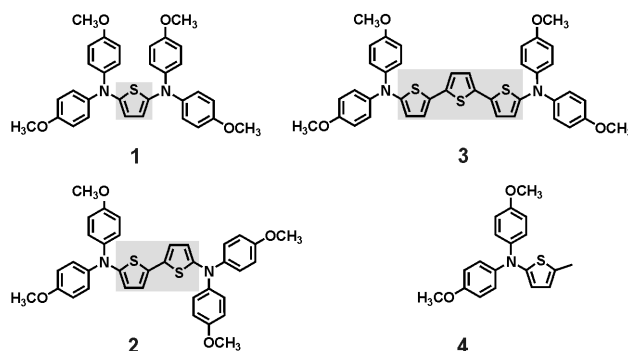
20 Electron transfer, organic mixed-valence, thiophene, molecular wires, intervalence charge transfer
21
22
23
24
25
26
27

28 INTRODUCTION

29
30
31
32
33 The one-electron oxidized forms of oligothiophenes exhibit a remarkable electrical conductivity, and
34 this property makes them well suited as hole transport materials in a variety of different (opto)electronic
35 applications.¹⁻⁵ Understanding distance-dependent charge delocalization in thiophene monocations is
36 therefore of significant interest. Numerous experimental and theoretical studies already explored the
37 electronic structure of oxidized thiophenes at a fundamental level, but mixed-valence approaches are
38 comparatively rare.⁶⁻¹⁴ In a purely computational study, Lacroix and coworkers arrived at the conclusion
39 that oligothiophene monocations may be described as organic mixed-valence species.¹⁵ Indeed, the one-
40 electron oxidized or one-electron reduced forms of several oligo-*p*-phenylene and oligo-*p*-phenylene
41 vinylene systems could be described well as organic mixed-valence compounds in various experimental
42 studies,¹⁶⁻²⁵ but until now there has been comparatively little conceptually analogous work on thiophene
43 systems.²⁶⁻³⁵ A notable exception is the recent study of the oxidized forms of bis(4-
44 (alkoxyphenyl)amino) derivatives of dithienylethene and bithiophene and the finding that a mixed-
45
46
47
48
49
50
51
52
53
54
55
56
57
58
59
60

valence description of these cations is meaningful.³⁶ Another exception is our own recent investigation of photoswitchable organic mixed-valence in dithienylethene systems.³⁷⁻³⁸

Scheme 1. Chemical structures of the molecules investigated in this work.



Here, we report on a detailed experimental investigation of the homologous series of α,α' -bis(diphenylamino)-substituted thiophene molecules (**1** – **3**) from Scheme 1. Further included into the study was a reference compound (**4**) comprised of a thiophene unit containing only one diphenylamino-substituent. From a combined electrochemical, optical spectroscopic and EPR study of the monocationic forms of these molecules we obtain detailed insight into charge-delocalization phenomena in thiophene monocations. Of key interest in this study was the question to which Robin/Day class the three monocations **1**⁺, **2**⁺, and **3**⁺ belong.³⁹ We anticipated that **1**⁺ would be a fully delocalized (class III) radical and wanted to explore whether the longer bithiophene (**2**⁺) and terthiophene (**3**⁺) systems would have a similar electronic structure, or whether there would be a transition to partial charge localization (class II) or even complete charge localization (class I).⁴⁰⁻⁴¹ For phenylene-bridged organic mixed valence systems this question had been answered previously,^{16, 19} but to the best of our knowledge such a length dependence of charge delocalization has not yet been investigated in a homologous series of thiophene-bridged organic mixed valence compounds.³⁴⁻³⁵ In view of the wide interest in thiophene materials mentioned above, it seemed relevant to explore over how many adjacent thiophene units an unpaired electron can be delocalized.

RESULTS AND DISCUSSION

Synthesis. Compound **1** was obtained using a palladium(0)-catalyzed reaction between 2,5-dibromothiophene and 4,4'-dimethoxydiphenylamine. The longer congeners (**2** and **3**) were synthesized in analogous manner using 5,5'-dibromo-2,2'-bithiophene and 5,5''-dibromo-2,2':5',2''-terthiophene as reaction partners with 4,4'-dimethoxydiphenylamine. Reference compound **4** was available from a prior investigation.³⁷ Detailed synthetic protocols and product characterization data for all new compounds are found in the Supporting Information.

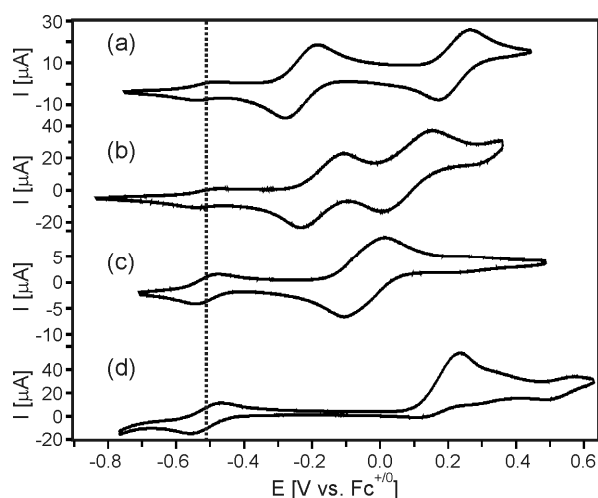


Figure 1. Cyclic voltammograms of the four compounds from Scheme 1 in dry and de-oxygenated acetonitrile measured in presence of 0.1 M tetrabutylammonium hexafluorophosphate (TBAPF₆) as a supporting electrolyte: (a) compound **1**; (b) compound **2**; (c) compound **3**; (d) compound **4**. The waves at -0.51 V vs. Fc⁺/Fc (dashed vertical line) are due to decamethylferrocene which was added for internal voltage calibration.

Electrochemistry. Figure 1 shows the results of cyclic voltammetry experiments with compounds **1** – **4** in de-oxygenated dry acetonitrile solution in presence of tetrabutylammonium hexafluorophosphate

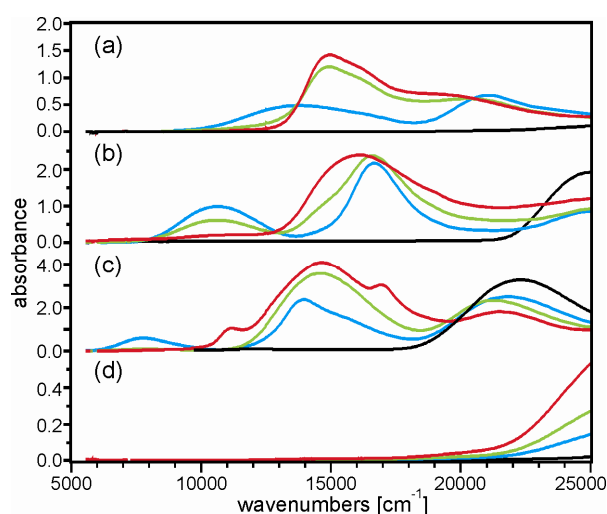
(TBAPF₆) as a supporting electrolyte. The waves at -0.51 V vs. Fc⁺/Fc (vertical dashed line) are due to decamethylferrocene which was added in small quantities as an internal reference for voltage calibration. The voltammograms of compounds **1** (Figure 1a) and **2** (Figure 1b) are comprised of two clearly discernable reversible waves which are separated by 450 mV and 250 mV, respectively, and they are attributed to one-electron oxidation processes involving predominantly the two different tertiary amino-groups. The decrease in the voltage splitting (ΔE) between the two waves from 450 mV in **1** to 250 mV in **2** is a manifestation of the increasing N-N distance and a decrease in electronic communication between the two redox-active moieties. For compound **3** only one reversible wave is observable at first glance, but digital fitting of the relevant part of the cyclic voltammogram from Figure 1c yields $\Delta E = 70$ mV (see Supporting Information). For reference compound **4** there is only one tertiary amino-group, hence the observation of a single oxidation wave in the potential range considered here is no surprise (Figure 1d). Moreover, this particular wave is irreversible, presumably due to electrochemically induced polymerization chemistry of the **4**⁺ species.

Table 1. Electrochemical potentials for one- and two-electron oxidation of the four compounds from Scheme 1 in Volts vs. Fc⁺/Fc. ΔE is the difference between the first ($E_{1/2}$ (1)) and the second oxidation potential ($E_{1/2}$ (2)) in mV, K_c is the comproportionation constant.

compound	$E_{1/2}$ (1)	$E_{1/2}$ (2)	ΔE [mV]	K_c
1	-0.23	0.22	450	$1.5 \cdot 10^9$
2	-0.17	0.08	250	$1.3 \cdot 10^5$
3	-0.08	-0.01	70	$1.5 \cdot 10^1$
4	0.16			

The electrochemical potentials for one- and two-electron oxidation of molecules **1** – **4** are summarized in Table 1. The fact that the first one-electron oxidation in the bis(diphenylamino)-systems occurs at

1 significantly more negative potentials than the first one-electron oxidation of reference compound **4** is
2 attributed to the more electron-rich nature of the twofold amino-substituted systems with respect to the
3 singly amino-substituted reference compound. We note that in the α,α' -bis(diphenylamino)-substituted
4 systems **1** – **3** the first oxidation potential ($E_{1/2}$ (1)) increases to more positive values with increasing
5 thiophene bridge length, while the second oxidation potential ($E_{1/2}$ (2)) is decreasing simultaneously to
6 more negative values.⁴² This leads to the abovementioned decrease in the overall oxidation potential
7 splitting (ΔE), which may be interpreted as a manifestation of decreasing electronic communication with
8 increasing length. In mixed-valence chemistry the comproportionation constant ($K_c = 10^{\Delta E/59 \text{ mV}}$) is often
9 used as a measure for the stability of the mixed-valence state,⁴³⁻⁴⁴ and we calculate values of $1.3 \cdot 10^9$ for
10 **1**⁺, $1.3 \cdot 10^5$ for **2**⁺, and $1.5 \cdot 10^1$ for **3**⁺ (Table 1). Classification of mixed-valence systems based on K_c
11 values is possible,³⁹ but requires some caution.^{43-44,45,46} With our thiophene systems from Scheme 1 we
12 are in the fortunate situation to have the possibility to gain complementary insight into the electronic
13 structures of the monocations by optical absorption and EPR spectroscopy. Therefore we refrain from
14 premature conclusions on the exclusive basis of the cyclic voltammetry studies.



36
37
38
39
40
41
42
43
44
45
46
47
48
49
50
51
52
Figure 2. Optical absorption spectra of the four compounds from Scheme 1 in acetonitrile solution in
53 presence of increasing amounts of $\text{Cu}(\text{ClO}_4)_2$ as a chemical oxidant: (a) compound **1**; (b) compound **2**;
54 (c) compound **3**; (d) compound **4**. Black lines: Neat compounds before adding any oxidant; blue lines:
55
56
57
58
59
60

1 after addition of 0.5 equivalents of oxidant; green traces: after addition of 1 equivalent of oxidant; red
2 traces: after addition of 2 equivalents of oxidant.
3
4
5
6
7

8 **Optical absorption spectroscopy.** The black traces in Figure 2 are the optical absorption spectra of
9 the charge-neutral forms of molecules **1** – **4** in acetonitrile solution at room temperature. The data shows
10 that none of the four compounds from Scheme 1 has any significant absorption features below 17000
11 cm^{-1} as long as the molecules are in their charge-neutral forms. Absorption spectra of molecules **1** – **4**
12 with extinction coefficients are shown in Figure S1 of the Supporting Information, and we find that the
13 lowest-energetic absorption maxima are at 29700 cm^{-1} for **1**, 25000 cm^{-1} for **2**, 22200 cm^{-1} for **3**, and
14 33300 cm^{-1} for **4**. Thus, there is a red-shift of the lowest absorption band with increasing thiophene
15 bridge length, which is likely a manifestation of increasing π -conjugation.⁴⁷⁻⁴⁹
16
17
18
19
20
21
22
23
24
25
26

27 The colored traces in Figure 2 were measured after addition of increasing amounts of copper(II)
28 perchlorate as an oxidant. The blue traces represent the spectra detected after addition of 0.5 equivalents,
29 the green traces are those measured after adding 1 equivalent, and the red traces are the spectra obtained
30 after 2 equivalents of $\text{Cu}(\text{ClO}_4)_2$ had been added. We note that in each of the three bis(dianisylamino)
31 systems (**1** – **3**; Figure 2a-c) absorption bands between 5000 and 15000 cm^{-1} appear upon oxidation.
32 Importantly, in each case the lowest energetic absorptions are only present in situations in which less
33 than 2 equivalents of oxidant have been added (blue and green traces), indicating that the respective
34 absorption bands are due to the one-electron oxidized (mixed-valence) species. The absence of any low-
35 energy absorptions in the oxidized forms of reference molecule **4** (Figure 2d) is consistent with the
36 interpretation of the lowest energy absorptions of **1**⁺, **2**⁺, and **3**⁺ as intervalence absorption bands.
37 However, we also note that (at least in cyclic voltammetry, vide supra) compound **4** undergoes
38 irreversible oxidation.
39
40
41
42
43
44
45
46
47
48
49
50
51
52
53
54

55 Figure 3 shows the lowest energetic absorptions of the monocations in more detail and on a properly
56 calibrated extinction scale. For this purpose, the low-energy portions of the optical absorption spectra
57
58
59
60

measured after addition of 0.25 equivalents of oxidant were employed. The use of data obtained in presence of a shortfall of chemical oxidant is a common procedure to avoid disproportionation of the mixed-valence state.³⁶ The black traces in Figure 3 represent the actual experimental data. While 1^+ has only one absorption band in the relevant spectral range (Figure 3a), the longer congeners (2^+ in Figure 3b and 3^+ in Figure 3c) exhibit two bands, and the reference compound (4^+) is spectroscopically innocent (Figure 3d). By analogy to prior investigations on bithiophene and dithienyl systems with diphenylamino-substituents it appears plausible to interpret the lowest energetic bands in $1^+ - 3^+$ as intervalence absorptions.^{36-37,50} Indeed, these absorptions fall into the spectral range in which intervalence absorptions of bis(triarylamine) radical cations are commonly observed.^{16, 20, 34-35, 51-61} An important difference to the intervalence absorptions of coordination compounds^{40, 62-65} are the comparatively large extinction coefficients of these bands, but this is a (favorable) peculiarity of organic mixed-valence compounds which has been noted many times before.³⁴⁻³⁵

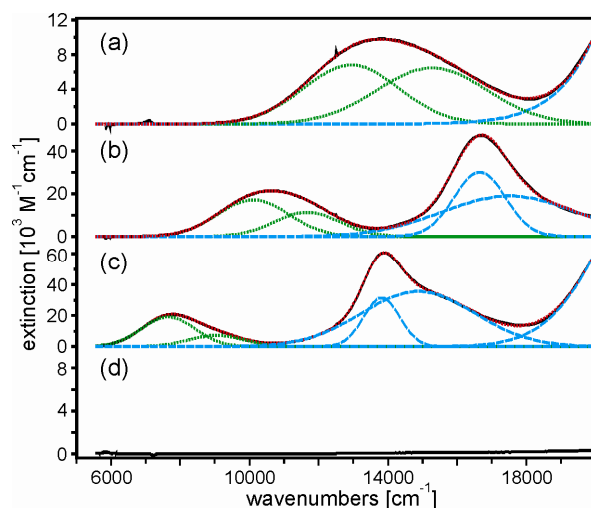


Figure 3. Black traces: Low-energy portions of the optical absorption spectra of the monocationic forms of the molecules from Scheme 1: (a) 1^+ ; (b) 2^+ ; (c) 3^+ ; (d) 4^+ . Colored traces: Gaussian fits to the experimental data. The parameters of the Gaussian functions represented by the dotted green traces are reported in Table 2.

In order to perform a quantitative analysis of the intervalence absorptions, the experimental spectra in Figure 3 were fitted to Gaussian functions. Due to the increasing complexity of the absorption spectra along the series $1^+ < 2^+ < 3^+$ an increasing number of Gaussians was required to obtain satisfactory fits: Three Gaussians were sufficient for Figure 3a, 4 were needed for the spectrum in Figure 3b, and 5 were necessary in the case of the spectrum in Figure 3c. In all cases the lowest energetic absorption band had to be fitted with two Gaussian functions (dashed green traces). The characteristics of the respective Gaussian functions are summarized in Table 2: ν_{\max,G_i} is the energetic position of the maximum of the i -th Gaussian while $\nu_{1/2,G_i}$ is its full width at half maximum. Given the fact that all of the lowest energetic absorptions have to be fitted by two Gaussian functions it is obvious that the shapes of these bands are asymmetric, an observation that is commonly made for class III systems or mixed-valence compounds that are near the borderline of class II and class III.^{16, 36, 63, 66} In order to capture the asymmetry of an intervalence band in one single number, it is customary to determine the bandwidth on the high-energy side of the intervalence band ($\nu_{1/2 [\text{high}]}$ in Table 2) as well as on its low-energy side ($\nu_{1/2 [\text{low}]}$ in Table 2), and to build the ratio between the two measures. In our specific cases this procedure yields $\nu_{1/2 [\text{high}]} / \nu_{1/2 [\text{low}]}$ ratios between 1.16 and 1.36 (fourth column of Table 2), which are typical values for systems near the borderline of class II and class III.^{16, 36, 63, 66}

Table 2. Parameters obtained from analysis of the lowest-energetic near-infrared absorptions in Figure 3: Twice the bandwidth on the high-energy side of the lowest absorption ($\nu_{1/2 [\text{high}]}$), twice the bandwidth on the low-energy side of the lowest absorption ($\nu_{1/2 [\text{low}]}$), and ratio between the two ($\nu_{1/2 [\text{high}]} / \nu_{1/2 [\text{low}]}$). $\nu_{\max,G1}$ and $\nu_{\max,G2}$ are the energetic positions of the maxima of the two Gaussian functions required to fit the lowest-energetic near-infrared absorption. $\nu_{1/2,G1}$ and $\nu_{1/2,G2}$ are the full widths at half maximum of these two Gaussian fit functions. $\nu_{\text{class II}}$ is the bandwidth which is expected based on equation 4.

compound	$\nu_{1/2 [\text{high}]}$ [cm^{-1}]	$\nu_{1/2 [\text{low}]}$ [cm^{-1}]	$\nu_{1/2 [\text{high}]} /$ $\nu_{1/2 [\text{low}]}$	$\nu_{\max,G1}$ [cm^{-1}]	$\nu_{1/2,G1}$ [cm^{-1}]	$\nu_{\max,G2}$ [cm^{-1}]	$\nu_{1/2,G2}$ [cm^{-1}]	$\nu_{\text{class II}}$ [cm^{-1}]

1 ⁺	5700	4300	1.33	12945	3231	15276	3723	5656
2 ⁺	3550	3060	1.16	10112	2426	11671	2232	4953
3 ⁺	2640	1940	1.36	7652	1800	9051	1850	4237

There is no clear trend of $\nu_{1/2 \text{ [high]}}/\nu_{1/2 \text{ [low]}}$ along the series of compounds **1⁺**, **2⁺**, **3⁺**. One might expect the respective ratio to decrease as the systems get longer and the class II character of the relevant mixed-valence species increases. From the finding that $\nu_{1/2 \text{ [high]}}/\nu_{1/2 \text{ [low]}} \neq 1$ one can merely conclude that all three systems deviate from pure class II behavior but it seems impossible to draw any quantitative conclusions regarding the percentage of class III character.

From the Gaussian fits to the intervalence bands in Figure 3 it is possible to determine the dipole moment (μ_{ge}) associated with the intervalence transition by employing equation 1.⁶⁷⁻⁶⁸

$$\mu_{ge} = 0.09584 \cdot \sqrt{\frac{\int \varepsilon(\nu) \cdot d\nu}{\nu_{\max}}} \quad (\text{eq. 1})$$

Equation 1 yields the transition dipole moment in units of Debye and requires ν_{\max} and $\varepsilon(\nu)$ input values in units of cm^{-1} and $\text{M}^{-1} \text{cm}^{-1}$, respectively. Here, ν_{\max} represents the experimentally determined maximum of the intervalence absorptions (fourth column in Table 3) while the integral over $\varepsilon(\nu)$ was taken as the integral over the two Gaussians needed to fit the lowest-energetic near-infrared absorptions. Thus we obtain μ_{ge} values ranging from 5.7 D for **1⁺** to 7.8 for **3⁺** (Table 3).

Table 3. Nitrogen-nitrogen distance (d_{NN}),^a number of σ -bonds between nitrogen atoms (n_{σ}), and parameters extracted from the near-infrared absorption spectra of the monocations in Figure 3: Absorption band maximum (ν_{\max}), transition dipole moment (μ_{ge} , in units of Debye), and electronic coupling matrix elements (H_{AB}) calculated using different models (see text).

compound	$d_{\text{NN}} [\text{\AA}]^a$	n_{σ}	$\nu_{\max} [\text{cm}^{-1}]$	$\mu_{ge} [\text{D}]$	$H_{\text{AB}} [\text{cm}^{-1}]$	$H_{\text{AB}} [\text{cm}^{-1}]$	$H_{\text{AB}} [\text{cm}^{-1}]$
----------	--------------------------------	--------------	-------------------------------	-----------------------	----------------------------------	----------------------------------	----------------------------------

					class II	class II; $2/3 \cdot d_{NN}$	class III
1 ⁺	5.2	4	13850	5.7	3160	4790	6925
2 ⁺	9.1	7	10620	7.7	1870	2835	5310
3 ⁺	13.0	10	7770	7.8	970	1470	3885

^a Estimated from molecular modeling of the charge-neutral parent compounds.

The transition dipole moment μ_{ge} is in direct relation with the electronic coupling matrix element H_{AB} describing the electronic interaction between the two redox-active units of a mixed-valence species.⁶⁹ This direct relationship is captured by equation 2, which was used here to estimate H_{AB} on the basis of the experimentally determined μ_{ge} values.

$$H_{AB} = \frac{\mu_{ge} \cdot V_{\max}}{e \cdot R} \quad (\text{eq. 2})$$

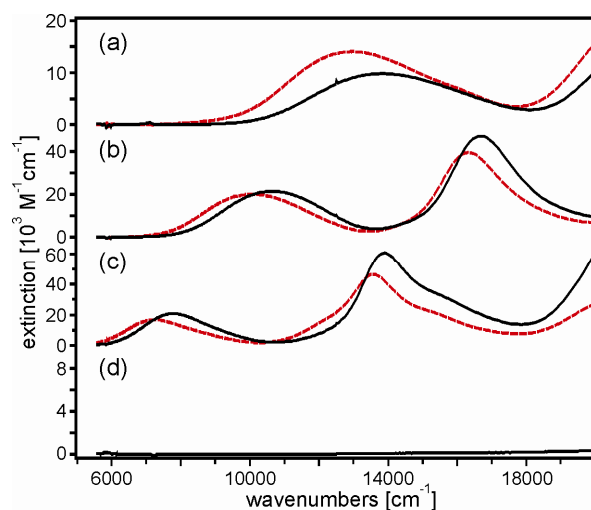
In equation 2, e is the elemental charge and R is the effective distance between redox centers. A question of central importance is usually what to take for R . The effective electron transfer distance can be substantially shorter than what might be expected from purely geometric considerations. For instance, the effective electron transfer distance in selected bis(triarylamine) mixed-valence systems has been found to be only roughly two thirds of the geometrical distance between nitrogen atoms,^{34, 61} and analogous investigations of mixed-valent dinitroaromatic anions have come to similar conclusions.⁷⁰⁻⁷¹ In principle it is possible to estimate R with various computational methods,⁷²⁻⁷⁶ but here we intend to rely exclusively on experimental observations. Therefore we give in Table 3 the results of two calculations with equation 2: Once we report H_{AB} calculated on the basis of the geometrical N-N distance (d_{NN} ; second column of Table 3), and once we give H_{AB} calculated on the basis of $R = 2/3 \cdot d_{NN}$. For compound **1⁺** we obtain $H_{AB} = 3160 \text{ cm}^{-1}$ (d_{NN}) and $H_{AB} = 4790 \text{ cm}^{-1}$ ($2/3 \cdot d_{NN}$). For reference, the *N,N,N',N'*-tetraanisyl-*p*-phenylenediamine monocation (TAPD⁺) has $H_{AB} = 3240 \text{ cm}^{-1}$, and this is a mixed-valence species which was classified as a borderline class II / class III system.¹⁶ For our systems we consider the analysis on the basis of $R = 2/3 \cdot d_{NN}$ more adequate than analysis based on $R = d_{NN}$, inter

1 alia because our EPR data (see below) suggests that there is significant unpaired spin density on the
2 thiophene bridges.
3

4 For class III systems, it is possible to estimate H_{AB} directly from the intervalence absorption band
5 maximum (ν_{\max}):
6
7

$$H_{AB} = \nu_{\max} / 2 \quad (\text{eq. 3})$$

8
9
10 The ν_{\max} values are given in the fourth column of Table 3 and using equation 3 one obtains H_{AB}
11 values of 6925 cm^{-1} (1^+), 5310 cm^{-1} (2^+), and 3885 cm^{-1} (3^+) (last column of Table 3). These are
12 relatively high H_{AB} values even when compared to some of the most strongly coupled organic mixed
13 valence systems known to date.³⁴⁻³⁵ For reference, the *N,N,N',N'*-tetramethyl-*p*-phenylene diamine
14 cation (Wurster's blue) has $H_{AB} \approx 8100 \text{ cm}^{-1}$, while *N,N,N',N'*-tetraanisyl-*p*-phenylene diamine cation
15 has $H_{AB} = 3240 \text{ cm}^{-1}$.³⁴⁻³⁵ Here we find H_{AB} values which are close to 4000 cm^{-1} even for the system
16 comprised of *three* adjacent thiophene units.
17
18
19
20
21
22
23
24
25
26
27
28
29
30



31
32
33
34
35
36
37
38
39
40
41
42
43
44
45
46
47
48 **Figure 4.** Optical absorption spectra of (a) 1^+ ; (b) 2^+ ; (c) 3^+ ; (d) 4^+ in acetonitrile (solid black traces) and
49 in dichloromethane (red traces).
50
51
52

53
54
55
56 When attempting to classify mixed-valence species according to the Robin and Day scheme,³⁹ the
57 solvent dependence of the intervalence absorptions may be helpful. We have therefore explored the
58
59
60

1 solvent dependence of the near-infrared absorptions of $\mathbf{1}^+$, $\mathbf{2}^+$, and $\mathbf{3}^+$, and the results of our efforts are
2 shown in Figure 4. Due to the poor solubility of our monocations in most common solvents, the solvent
3 dependence study remained restricted to acetonitrile (black traces) and dichloromethane (red traces). The
4 key observation is the same in all three cases: The lowest-energy absorption band is red-shifted when
5 going from acetonitrile to dichloromethane. However, the spectral shifts are relatively modest and range
6 from 850 cm^{-1} ($\mathbf{1}^+$) to 560 cm^{-1} ($\mathbf{3}^+$). For class II systems a red-shift upon solvent change from
7 acetonitrile to dichloromethane is to be expected because of a decrease of the solvent reorganization
8 energy, whereas for pure class III systems one would expect ν_{max} to be independent of solvent. In our
9 case there is a solvent dependence, but it is a comparatively weak one, suggesting that at least the shorter
10 members of our cations series ($\mathbf{1}^+$ and $\mathbf{2}^+$) are indeed near the borderline of class II and class III. The
11 comproportionation constants (K_c) calculated above ($1.3 \cdot 10^9$ for $\mathbf{1}^+$ and $1.3 \cdot 10^5$ for $\mathbf{2}^+$) do not contradict
12 this classification. For the longest congener ($\mathbf{3}^+$) the electrochemical data suggests class I ($K_c = 15$), but
13 the optical spectroscopic data is more consistent with borderline class II / class III. We note that
14 comproportionation constants have often been employed as measures for electronic couplings, but it has
15 been demonstrated that they can actually provide a poor guide and should be used with caution.⁷⁷
16 Therefore, we think that the optical absorption (and EPR) data are more reliable for classifying our
17 mixed-valence compounds.
18
19
20
21
22
23
24
25
26
27
28
29
30
31
32
33
34
35
36
37
38
39

40 An additional argument which supports interpretation of $\mathbf{2}^+$ and $\mathbf{3}^+$ as borderline class II / class III
41 systems is the relatively narrow width of the intervalence absorption bands observed for these
42 compounds: For a pure class II system one would expect the bandwidth to satisfy equation 4, but in the
43 present cases the calculated bandwidths ($\nu_{\text{class II}}$, last column of Table 2; 4953 cm^{-1} and 4237 cm^{-1}) are
44 significantly larger than the experimentally observed bandwidths ($\nu_{1/2 [\text{high}]}$, second column of Table 2;
45 3550 cm^{-1} , 2640 cm^{-1}).
46
47
48
49
50
51
52
53
54

$$\nu_{\text{class II}} = \sqrt{2310 \cdot \nu_{\text{max}}} \quad (\text{eq. 4})$$

1
2
3 **EPR spectroscopy.** Given the challenges in classifying the monocations 1^+ , 2^+ , 3^+ according to the
4 Robin and Day scheme based on electrochemical results and optical absorption spectroscopy, we
5 decided to perform EPR spectroscopy with these systems in order to gain complementary insight into
6 their electronic structures. Furthermore, EPR spectroscopy can potentially shed some light on the
7 question to what extent these monocations may indeed be considered diamino mixed-valence
8 compounds, or to what extent they have to be regarded as thiophene-bridge oxidized species.³⁶
9

10
11
12
13
14
15
16
17 The solid lines in the upper half of Figure 5 are the experimental X-band EPR spectra obtained at
18 room temperature from dilute dichloromethane solutions of 1^+ (a), 2^+ (b), and 3^+ (c). In all three cases,
19 the EPR signals are centered at a g-value of 2.005, which is typical for triarylamine radical cations.⁷⁸
20
21
22
23
24 The appearance of the spectra in Figure 5 resembles that observed for related bithiophene and
25 dithienylethene radicals which were end-capped with 4-alkoxyphenylamino groups;³⁶ the EPR spectrum
26 of 2^+ had even been reported before.³⁶ The hyperfine structure of our EPR spectra can be understood on
27 the basis of an interaction of the unpaired electron spin with the nuclear spins of ^{14}N ($I = 1$) and ^1H ($I =$
28 $1/2$), whereby the magnitudes of the coupling constants (for interaction with ^{14}N and ^1H) are similar.^{31,36}
29
30
31
32
33
34
35
36
37 This statement is corroborated by the simulated EPR spectra shown as dashed traces in the lower half of
38 Figure 5. In performing these simulations, we attempted to use a minimum of adjustable parameters. We
39 found that when going from 1^+ to 2^+ and finally to 3^+ , the experimental EPR data can only be simulated
40 satisfactorily when increasing the number of coupling constants along this series of radicals (Table 4).
41
42
43
44
45
46
47
48
49
50
51
52
53
54
55
56
57
58
59
60

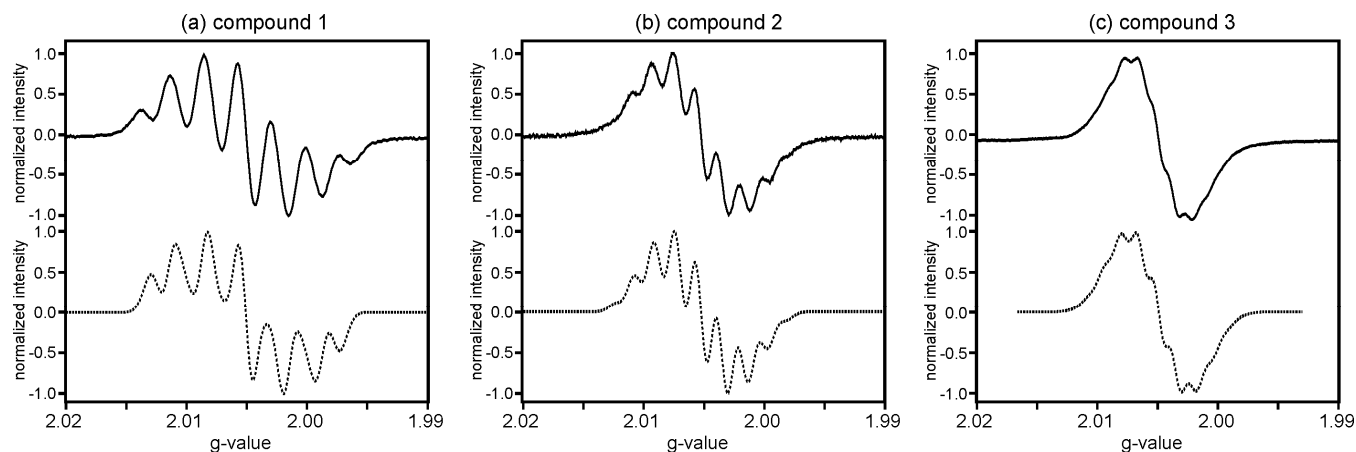


Figure 5. Solid traces: Experimental X-band EPR spectra obtained from radicals 1^+ (a), 2^+ (b), 3^+ (c) in dilute dichloromethane solution at room temperature. Dashed traces: Simulated EPR spectra using the hyperfine coupling parameters given in Table 4. The simulations occurred using the WINEPR SimFonia Software.

Table 4. Hyperfine coupling constants (in units of Gauss) used to simulate the experimental X-band EPR spectra represented by the solid traces in the upper half of Figure 5. The dashed lines in the lower half of Figure 5 illustrate the outcomes of these simulations.

radical	a_N [G]	a_H [G]	$a_{H'}$ [G]	$a_{H''}$ [G]
1^+	4.3	2.6		
2^+	2.9	2.4	2.0	
3^+	2.2	2.1	2.0	1.8

For 1^+ , it is sufficient to invoke coupling to two nitrogen nuclei with a hyperfine coupling constant $a_N = 4.3$ G and simultaneous coupling to two hydrogen nuclei with $a_H = 2.6$ G. In other words, the experimental data for 1^+ is in line with uniform spin distribution over the entire molecule, consistent with class III mixed-valence behavior on the EPR timescale. This observation is similar to what has been reported for other bis(triarylamine) radical cations.^{31, 36, 60-61} It appears plausible that the two

1 chemically equivalent hydrogen nuclei which couple to the unpaired electron spin with $a_H = 2.6$ G are in
2 fact those attached to the thiophene bridging unit of molecule **1**.⁷⁹

3
4
5 The experimental EPR spectrum of **2**⁺ in Figure 5b can be simulated using three different hyperfine
6 coupling constants: $a_N = 2.9$ G, $a_H = 2.4$ G and $a_{H'} = 2.0$ G (third row of Table 4). Importantly, all of
7 these couplings involve two equivalent nuclei, suggesting that the electron is again symmetrically
8 delocalized on the EPR timescale. The additional hydrogen hyperfine constant in this case ($a_{H'}$) is most
9 likely due to the fact that there are now two chemically distinct hydrogen atoms attached to the
10 thiophene bridge; indeed, this interpretation is in line with a prior experimental and theoretical study of
11 **2**⁺ and a series of related thiophene cations.³⁶

12
13
14 For radical **3**⁺, four hyperfine coupling constants must be invoked (fourth line of Table 4), namely one
15 for two equivalent nitrogen atoms ($a_N = 2.2$), and three for pairs of equivalent hydrogen nuclei ($a_H = 2.1$
16 G, $a_{H'} = 2.0$ G, $a_{H''} = 1.8$ G). In analogy to the shorter **1**⁺ and **2**⁺ radicals, the EPR simulation in Figure
17 5c thus leads us to the conclusion that the unpaired electron spin is symmetrically delocalized over the
18 **3**⁺ species on the EPR timescale.

19
20
21 From the EPR spectra alone, one would thus arrive at the conclusion that **1**⁺, **2**⁺, and **3**⁺ are all class III
22 mixed-valence species. However, it is to be noted that even class II compounds can in principle exhibit
23 EPR spectra that suggest complete delocalization of the unpaired electron spin.³⁴ Specifically, this is the
24 case in systems in which thermal electron transfer between the two ends of the molecule is rapid on the
25 EPR timescale, i. e., faster than $\sim 10^{-7}$ s. There have been several comparative investigations of optical
26 and thermal electron transfer in organic mixed-valence systems (mostly on bis(hydrazine) radical
27 cations),⁸⁰⁻⁸² which have come to the conclusion that the results obtained by the two fundamentally
28 different experimental techniques (i. e., optical absorption and EPR spectroscopy) need not necessarily
29 lead to the same conclusion, mostly because these techniques probe electron transfer on significantly
30 different timescales. Be that as it may, in our specific case the EPR data is consistent with the optical
31 absorption results in that both sets of data can be analyzed adequately by assuming complete (in EPR) or
32 nearly complete (in absorption) delocalization of the unpaired electron.

1 On a final note in this section we point out that the hyperfine constant for coupling to the two
2 equivalent nitrogen nuclei decreases from $a_N = 4.3$ G in $\mathbf{1}^+$ to $a_N = 2.9$ G in $\mathbf{2}^+$, and finally to $a_N = 2.2$ G
3 in $\mathbf{3}^+$. It appears plausible that this decrease is a manifestation of increasing spin delocalization away
4 from the nitrogen atoms towards the center of the thiophene bridge. The expected increase in π -
5 conjugation with increasing thiophene bridge length seems compatible with this interpretation.^{95,83}
6
7
8
9
10
11
12
13
14
15
16

17 SUMMARY AND CONCLUSIONS

18
19
20
21 One of the key findings from the research presented in this paper is that a mixed-valence description
22 of α,α -bis(dianisylamino)-substituted thiophene monocations is meaningful from an experimental point
23 of view, as suggested by the theoretical work performed by Lacroix and coworkers.¹⁵ Our experimental
24 work demonstrates that the mixed-valence approach is in fact reasonable for analysis of electrochemical,
25 optical absorption and EPR spectroscopic data obtained from amine-decorated thiophene monocations.
26
27
28
29
30
31
32

33 The optical absorption and EPR data is consistent with interpretation of the $\mathbf{1}^+$, $\mathbf{2}^+$, and $\mathbf{3}^+$ radical
34 species as strongly delocalized systems: EPR spectroscopy suggests them to be class III systems, while
35 optical absorption spectroscopy is compatible with interpretation both as class III and borderline class II
36 / class III species. The computational work by Lacroix and coworkers clearly shows that a transition
37 between different Robin-Day classes is expected for long oligothiophenes.¹⁵ Our current experimental
38 study suggests that this is the case only for molecules comprised of more than three adjacent thiophene
39 units.
40
41
42
43
44
45
46
47
48
49
50
51
52
53
54
55
56
57
58
59
60

EXPERIMENTAL SECTION

1
2
3
4
5 Synthetic protocols and product characterization data for **1**, **2**, **3**, and all relevant isolable reaction
6 intermediates are provided in the Supporting Information. ^1H and ^{13}C NMR spectroscopy was performed
7 using Bruker Avance DRX300 and Bruker B-ACS-120 instruments, electron-ionization mass
8 spectrometry (EI-MS) occurred on a Finnigan MAT8200 instrument, and elemental analyzes were
9 conducted on a Vario EL III CHNS analyzer from Elementar. Chemical oxidation of the charge-neutral
10 molecules from Scheme 1 to their mono- and dicationic forms was effected with $\text{Cu}(\text{ClO}_4)_2$, which
11 represents a standard procedure for generating triarylamine radical cations.^{37, 84-85} Cyclic voltammetry
12 was performed using a potentiostat from Princeton Applied Research (Versastat3-200) with a glassy
13 carbon disk working electrode and two separate silver wires as counter and quasi-reference electrodes.
14 Optical absorption spectra were measured on a Cary 5000 instrument from Varian. The EPR spectra
15 were recorded on a ELEXSYS CW-EPR spectrometer E500 from Bruker, using a microwave frequency
16 of about 9.42 GHz. The modulation frequency was 100 KHz, the modulation amplitude was $1 \times 10^{-4}\text{G}$,
17 and the power of the microwave 5-6 mW. The spectrometer is equipped with a digital temperature
18 control system ER 4131 VT, covering a temperature range from 110 to 350K. UV-vis and cyclic
19 voltammetry data was analyzed using the Igor Pro software (version 6.0.0.0) from WaveMetrics.
20
21
22
23
24
25
26
27
28
29
30
31
32
33
34
35
36
37
38
39
40
41
42
43

ACKNOWLEDGMENT

44
45
46
47
48
49 Financial support from the Deutsche Forschungsgemeinschaft (DFG) through grant number
50 WE4815/1-1 is gratefully acknowledged. We are grateful for financial support for the research visit of
51 Palas Baran Pati from the International Office, University of Göttingen.
52
53
54
55
56
57
58
59
60

SUPPORTING INFORMATION

Synthetic protocols and characterization data for molecules **1** - **3** and all intermediate reaction products. Additional optical absorption data. Digital fit of the cyclic voltammogram from Figure 1c.

This material is available free of charge via the Internet at <http://pubs.acs.org>.

REFERENCES

- (1) Roncali, J., *Chem. Rev.* **1992**, *92*, 711-738.
- (2) Horowitz, G., *Adv. Mater.* **1998**, *10*, 365-377.
- (3) Murphy, A. R.; Frechet, J. M. J., *Chem. Rev.* **2007**, *107*, 1066-1096.
- (4) Zhu, X. H.; Peng, J. B.; Caoa, Y.; Roncali, J., *Chem. Soc. Rev.* **2011**, *40*, 3509-3524.
- (5) Ma, C. Q.; Pisula, W.; Weber, C.; Feng, X. L.; Müllen, K.; Bäuerle, P., *Chem.-Eur. J.* **2011**, *17*, 1507-1518.
- (6) Miller, L. L.; Mann, K. R., *Acc. Chem. Res.* **1996**, *29*, 417-423.
- (7) Katz, H. E.; Bao, Z., *J. Phys. Chem. B* **2000**, *104*, 671-678.
- (8) Katz, H. E.; Bao, Z. N.; Gilat, S. L., *Acc. Chem. Res.* **2001**, *34*, 359-369.
- (9) Hutchison, G. R.; Ratner, M. A.; Marks, T. J., *J. Phys. Chem. B* **2005**, *109*, 3126-3138.
- (10) Hutchison, G. R.; Ratner, M. A.; Marks, T. J., *J. Am. Chem. Soc.* **2005**, *127*, 16866-16881.
- (11) James, D. K.; Tour, J. M., Molecular wires. In *Molecular Wires: From Design to Properties*, De Cola, L., Ed. Springer-Verlag Berlin: Berlin, 2005; Vol. 257, pp 33-62.

- 1
2
3
4
5
6
7
8
9
10
11
12
13
14
15
16
17
18
19
20
21
22
23
24
25
26
27
28
29
30
31
32
33
34
35
36
37
38
39
40
41
42
43
44
45
46
47
48
49
50
51
52
53
54
55
56
57
58
59
60
- (12) Gao, P.; Beckmann, D.; Tsao, H. N.; Feng, X. L.; Enkelmann, V.; Baumgarten, M.; Pisula, W.; Müllen, K., *Adv. Mater.* **2009**, *21*, 213-216.
- (13) Zade, S. S.; Zamoshchik, N.; Bendikov, M., *Acc. Chem. Res.* **2011**, *44*, 14-24.
- (14) Speck, M. J.; Schaarschmidt, D.; H., L., *Organometallics* **2012**, *31*, 1975-1982.
- (15) Lacroix, J. C.; Chane-Ching, K. I.; Maquère, F.; Maurel, F., *J. Am. Chem. Soc.* **2006**, *128*, 7264-7276.
- (16) Lambert, C.; Nöll, G., *J. Am. Chem. Soc.* **1999**, *121*, 8434-8442.
- (17) Rovira, C.; Ruiz-Molina, D.; Elsner, O.; Vidal-Gancedo, J.; Bonvoisin, J.; Launay, J.-P.; Veciana, J., *Chem. Eur. J.* **2001**, *7*, 240-250.
- (18) Lindeman, S. V.; Rosokha, S. V.; Sun, D.; Kochi, J. K., *J. Am. Chem. Soc.* **2002**, *124*, 843-855.
- (19) Rosokha, S. V.; Sun, D.-L.; Kochi, J. K., *J. Phys. Chem. A* **2002**, *106*, 2283-2292.
- (20) Barlow, S.; Risko, C.; Chung, S. J.; Tucker, N. M.; Coropceanu, V.; Jones, S. C.; Levi, Z.; Brédas, J. L.; Marder, S. R., *J. Am. Chem. Soc.* **2005**, *127*, 16900-16911.
- (21) Funston, A.; Kirby, J. P.; Miller, J. R.; Pospíšil, L.; Fiedler, J.; Hromadová, M.; Gál, M.; Pecka, J.; Valášek, M.; Zawada, Z.; Rempala, P.; Michl, J., *J. Phys. Chem. A* **2005**, *109*, 10862-10869.
- (22) Nelsen, S. F.; Weaver, M. N.; Telo, J. P., *J. Phys. Chem. A* **2007**, *111*, 10993-10997.
- (23) Zhou, G.; Baumgarten, M.; Müllen, K., *J. Am. Chem. Soc.* **2007**, *129*, 12211-12221.
- (24) Nelsen, S. F.; Weaver, M. N.; Telo, J. P., *J. Am. Chem. Soc.* **2007**, *129*, 7036-7043.
- (25) Lloveras, V.; Vidal-Gancedo, J.; Figueira-Duarte, T. M.; Nierengarten, J. F.; Novoa, J. J.; Mota, F.; Ventosa, N.; Rovira, C.; Veciana, J., *J. Am. Chem. Soc.* **2011**, *133*, 5818-5833.

- 1 (26) Bäuerle, P.; Segelbacher, U.; Maier, A.; Mehring, M., *J. Am. Chem. Soc.* **1993**, *115*, 10217-
2 10223.
3
4
5
6 (27) Zhu, Y. B.; Wolf, M. O., *J. Am. Chem. Soc.* **2000**, *122*, 10121-10125.
7
8
9 (28) Le Stang, S.; Paul, F.; Lapinte, C., *Organometallics* **2000**, *19*, 1035-1043.
10
11
12 (29) Fraysse, S.; Coudret, C.; Launay, J.-P., *J. Am. Chem. Soc.* **2003**, *125*, 5880-5888.
13
14
15 (30) Casado, J.; Gonzalez, S. R.; Delgado, M. C. R.; Oliva, M. M.; Navarrete, J. T. L.; Caballero, R.;
16 de la Cruz, P.; Langa, F., *Chem.-Eur. J.* **2009**, *15*, 2548-2559.
17
18
19
20
21 (31) Rohde, D.; Dunsch, L.; Tabet, A.; Hartmann, H.; Fabian, J., *J. Phys. Chem. B* **2006**, *110*, 8223-
22 8231.
23
24
25
26 (32) Gao, L. B.; Kan, J.; Fan, Y.; Zhang, L. Y.; Liu, S. H.; Chen, Z. N., *Inorg. Chem.* **2007**, *46*, 5651-
27 5664.
28
29
30
31
32 (33) Nöll, G.; Avola, M.; Lynch, M.; Daub, J., *J. Phys. Chem. C* **2007**, *111*, 3197-3204.
33
34
35
36 (34) Hankache, J.; Wenger, O. S., *Chem. Rev.* **2011**, *111*, 5138-5178.
37
38
39 (35) Heckmann, A.; Lambert, C., *Angew. Chem. Int. Ed.* **2012**, *51*, 326-392.
40
41
42 (36) Odom, S. A.; Lancaster, K.; Beverina, L.; Lefler, K. M.; Thompson, N. J.; Coropceanu, V.;
43 Brédas, J. L.; Marder, S. R.; Barlow, S., *Chem. Eur. J.* **2007**, *13*, 9637-9646.
44
45
46
47 (37) He, B.; Wenger, O. S., *J. Am. Chem. Soc.* **2011**, *133*, 17027-17036.
48
49
50
51 (38) Wenger, O. S., *Chem. Soc. Rev.* **2012**, *41*, 3772-3779.
52
53
54 (39) Robin, M. B.; Day, P., *Adv. Inorg. Chem. Radiochem.* **1967**, *10*, 247-422.
55
56
57 (40) Brunshwig, B. S.; Creutz, C.; Sutin, N., *Chem. Soc. Rev.* **2002**, *31*, 168-184.
58
59
60

- 1
2
3
4
5
6
7
8
9
10
11
12
13
14
15
16
17
18
19
20
21
22
23
24
25
26
27
28
29
30
31
32
33
34
35
36
37
38
39
40
41
42
43
44
45
46
47
48
49
50
51
52
53
54
55
56
57
58
59
60
- (41) Creutz, C., *Prog. Inorg. Chem.* **1983**, *30*, 1-73.
- (42) The separation between the cathodic and anodic peaks in Figure 1 is significantly larger than 59 mV; the precise reasons for this are unclear.
- (43) D'Alessandro, D. M.; Keene, F. R., *Dalton Trans.* **2004**, 3950-3954.
- (44) Kaim, W.; Klein, A.; Glöckle, M., *Acc. Chem. Res.* **2000**, *33*, 755-763.
- (45) One difficulty with using K_c values for characterizing mixed-valence behavior arises from the fact that calculation of the comproportionation constant relies on the assumption that the solvation energies for mono- and dications is identical. However, this does not necessarily have to be the case, see for example ref. 46.
- (46) Nelsen, S. F., *Adv. Phys. Org. Chem.* **2006**, *41*, 183-215.
- (47) Jones, D.; Guerra, M.; Favaretto, L.; Modelli, A.; Fabrizio, M.; Distefano, G., *J. Phys. Chem.* **1990**, *94*, 5761-5766.
- (48) da Silva, D. A.; Coropceanu, V.; Fichou, D.; Gruhn, N. E.; Bill, T. G.; Gierschner, J.; Cornil, J.; Brédas, J. L., *Philos. Trans. R. Soc. A* **2007**, *365*, 1435-1452.
- (49) Salzner, U., *J. Phys. Chem. A* **2010**, *114*, 10997-11007.
- (50) In using the term “intervalence” we do not intend to make a distinction between partially and fully charge-delocalized systems. As is common practice, we use this term interchangeably for class II and class III mixed valence compounds.
- (51) Lambert, C.; Nöll, G., *Angew. Chem. Int. Ed.* **1998**, *37*, 2107-2110.
- (52) Bonvoisin, J.; Launay, J. P.; Van der Auweraer, M.; De Schryver, F. C., *J. Phys. Chem.* **1994**, *98*, 5052-5057.

- 1 (53) Bonvoisin, J.; Launay, J. P.; Verbouwe, W.; Van der Auweraer, M.; De Schryver, F. C., *J. Phys.*
2
3 *Chem.* **1996**, *100*, 17079-17082.
4
5
6 (54) Coropceanu, V.; Lambert, C.; Nöll, G.; Brédas, J. L., *Chem. Phys. Lett.* **2003**, *373*, 153-160.
7
8
9 (55) Jones, S. C.; Coropceanu, V.; Barlow, S.; Kinnibrugh, T.; Timofeeva, T.; Brédas, J. L.; Marder,
10
11 S. R., *J. Am. Chem. Soc.* **2004**, *126*, 11782-11783.
12
13
14 (56) Sun, D.; Rosokha, S. V.; Kochi, J. K., *Angew. Chem. Int. Ed.* **2005**, *44*, 5133-5136.
15
16
17 (57) Barlow, S.; Risko, C.; Coropceanu, V.; Tucker, N. M.; Jones, S. C.; Levi, Z.; Khrustalev, V. N.;
18
19 Antipin, M. Y.; Kinnibrugh, T. L.; Timofeeva, T.; Marder, S. R.; Brédas, J. L., *Chem. Commun.* **2005**,
20
21 764-766.
22
23
24
25 (58) Nöll, G.; Avola, M., *J. Phys. Org. Chem.* **2006**, *19*, 238-241.
26
27
28 (59) Amthor, S.; Lambert, C., *J. Phys. Chem. A* **2006**, *110*, 1177-1189.
29
30
31 (60) Kattnig, D. R.; Mladenova, B.; Grampp, G.; Kaiser, C.; Heckmann, A.; Lambert, C., *J. Phys.*
32
33 *Chem. C* **2009**, *113*, 2983-2995.
34
35
36
37 (61) Lancaster, K.; Odom, S. A.; Jones, S. C.; Thayumanavan, S.; Marder, S. R.; Brédas, J. L.;
38
39 Coropceanu, V.; Barlow, S., *J. Am. Chem. Soc.* **2009**, *131*, 1717-1723.
40
41
42 (62) Brunshwig, B. S.; Sutin, N., *Coord. Chem. Rev.* **1999**, *187*, 233-254.
43
44
45 (63) Demadis, K. D.; Hartshorn, C. M.; Meyer, T. J., *Chem. Rev.* **2001**, *101*, 2655-2685.
46
47
48 (64) D'Alessandro, D. M.; Keene, F. R., *Chem. Soc. Rev.* **2006**, *35*, 424-440.
49
50
51 (65) D'Alessandro, D. M.; Keene, F. R., *Chem. Rev.* **2006**, *106*, 2270-2298.
52
53
54 (66) Nelsen, S. F., *Chem. Eur. J.* **2000**, *6*, 581-588.
55
56
57 (67) Creutz, C.; Newton, M. D.; Sutin, N., *J. Photochem. Photobiol. A* **1994**, *82*, 47-59.
58
59
60

- 1
2
3
4
5
6
7
8
9
10
11
12
13
14
15
16
17
18
19
20
21
22
23
24
25
26
27
28
29
30
31
32
33
34
35
36
37
38
39
40
41
42
43
44
45
46
47
48
49
50
51
52
53
54
55
56
57
58
59
60
- (68) Cave, R. J.; Newton, M. D., *Chem. Phys. Lett.* **1996**, *249*, 15-19.
- (69) Hush, N. S., *Prog. Inorg. Chem.* **1967**, *8*, 391.
- (70) Nelsen, S. F.; Konradsson, A. E.; Weaver, M. N.; Telo, J. P., *J. Am. Chem. Soc.* **2003**, *125*, 12493-12501.
- (71) Nelsen, S. F.; Weaver, M. N.; Zink, J. I.; Telo, J. P., *J. Am. Chem. Soc.* **2005**, *127*, 10611-10622.
- (72) Nelsen, S. F.; Newton, M. D., *J. Phys. Chem. A* **2000**, *104*, 10023-10031.
- (73) Johnson, R. C.; Hupp, J. T., *J. Am. Chem. Soc.* **2001**, *123*, 2053-2057.
- (74) Coropceanu, V.; Malagoli, M.; André, J. M.; Brédas, J. L., *J. Am. Chem. Soc.* **2002**, *124*, 10519-10530.
- (75) Renz, M.; Theilacker, K.; Lambert, C.; Kaupp, M., *J. Am. Chem. Soc.* **2009**, *131*, 16292-16302.
- (76) Kaupp, M.; Renz, M.; Parthey, M.; Stolte, M.; Würthner, F.; Lambert, C., *Phys. Chem. Chem. Phys.* **2011**, *13*, 16973-16986.
- (77) Barrière, F.; Camire, N.; Geiger, W. E.; Mueller-Westerhoff, U. T.; Sanders, R., *J. Am. Chem. Soc.* **2002**, *124*, 7262-7263.
- (78) Bamberger, S.; Hellwinkel, D.; Neugebauer, F. A., *Chem. Ber.* **1975**, *108*, 2416-2421.
- (79) DFT calculations could potentially shed more light on this issue, but this is beyond the scope of our detailed experimental study.
- (80) Nelsen, S. F.; Ismagilov, R. F.; Trieber, D. A., *Science* **1997**, *278*, 846-849.
- (81) Nelsen, S. F.; Chang, H.; Wolff, J. J.; Adamus, J., *J. Am. Chem. Soc.* **1993**, *115*, 12276-12289.
- (82) Nelsen, S. F.; Ismagilov, R. F.; Powell, D. R., *J. Am. Chem. Soc.* **1996**, *118*, 6313-6314.

1 (83) Jenart, M.; Niebel, C.; Balandier, J. Y.; Leroy, J.; Mignolet, A.; Stas, S.; Van Vooren, A.; Cornil,
2 J.; Geerts, Y. H., *Tetrahedron* **2012**, *68*, 349-355.
3

4
5 (84) Sreenath, K.; Suneesh, C. V.; Gopidas, K. R.; Flowers, R. A., *J. Phys. Chem. A* **2009**, *113*, 6477-
6 6483.
7
8

9
10 (85) Sreenath, K.; Thomas, T. G.; Gopidas, K. R., *Org. Lett.* **2011**, *13*, 1134-1137.
11
12
13
14
15
16
17
18
19
20
21
22
23
24
25
26
27
28
29
30
31
32
33
34
35
36
37
38
39
40
41
42
43
44
45
46
47
48
49
50
51
52
53
54
55
56
57
58
59
60

SYNOPSIS TOC

